






# Feasibility of Velocity-Selective Arterial Spin Labeling in Breast Cancer Patients for Noncontrast-Enhanced Perfusion Imaging

Suzanne L. Franklin, MSc,<sup>1,2,3\*</sup>  Nora Voormolen, MD,<sup>4</sup> Isabell K. Bones, MSc,<sup>2</sup>   
Tijmen Korteweg, MD, PhD,<sup>4</sup> Martin N. J. M. Wasser, MD,<sup>4</sup> Henrike G. Dankers, BSc,<sup>4</sup>  
Daniele Cohen, MD, PhD,<sup>5</sup> Marijn van Stralen, PhD,<sup>2</sup>  Clemens Bos, PhD,<sup>2</sup>  and  
Matthias J. P. van Osch, PhD<sup>1,3</sup> 

**Background:** Dynamic contrast-enhanced (DCE) MRI is the most sensitive method for detection of breast cancer. However, due to high costs and retention of intravenously injected gadolinium-based contrast agent, screening with DCE-MRI is only recommended for patients who are at high risk for developing breast cancer. Thus, a noncontrast-enhanced alternative to DCE is desirable.

**Purpose:** To investigate whether velocity selective arterial spin labeling (VS-ASL) can be used to identify increased perfusion and vascularity within breast lesions compared to surrounding tissue.

**Study Type:** Prospective.

**Population:** Eight breast cancer patients.

**Field Strength/Sequence:** A 3 T; VS-ASL with multislice single-shot gradient-echo echo-planar-imaging readout.

**Assessment:** VS-ASL scans were independently assessed by three radiologists, with 3–25 years of experience in breast radiology. Scans were scored on lesion visibility and artifacts, based on a 3-point Likert scale. A score of 1 corresponded to “lesions being distinguishable from background” (lesion visibility), and “no or few artifacts visible, artifacts can be distinguished from blood signal” (artifact score). A distinction was made between mass and nonmass lesions (based on BI-RADS lexicon), as assessed in the standard clinical exam.

**Statistical Tests:** Intra-class correlation coefficient (ICC) for interobserver agreement.

**Results:** The ICC was 0.77 for lesion visibility and 0.84 for the artifact score. Overall, mass lesions had a mean score of 1.27 on lesion visibility and 1.53 on the artifact score. Nonmass lesions had a mean score of 2.11 on lesion visibility and 2.11 on the artifact score.

**Data Conclusion:** We have demonstrated the technical feasibility of bilateral whole-breast perfusion imaging using VS-ASL in breast cancer patients.

**Evidence Level:** 1

**Technical Efficacy:** Stage 1

J. MAGN. RESON. IMAGING 2021;54:1282–1291.

BREAST MRI is the most sensitive tool for detection of breast cancer<sup>1</sup> with a sensitivity at least twice as high as mammography.<sup>1</sup> The specificity of breast MRI is increased by use of multiparametric (mpMRI) protocols,<sup>2</sup> which combine information from different MR techniques.<sup>2</sup> It is recommended as an annual screening tool for women with an increased risk of breast cancer.<sup>3–5</sup> The backbone of breast MRI is dynamic contrast-enhanced (DCE) MRI, which relies on intravenous injection of a

View this article online at [wileyonlinelibrary.com](http://wileyonlinelibrary.com). DOI: 10.1002/jmri.27781

Received Feb 4, 2021, Accepted for publication Jun 1, 2021.

\*Address reprint requests to: S.L.F., Albinusdreef 2, 2333 ZA Leiden, The Netherlands. E-mail: [s.l.franklin@lumc.nl](mailto:s.l.franklin@lumc.nl)

From the <sup>1</sup>C.J. Gorter Center for High Field MRI, Department of Radiology, Leiden University Medical Center, Leiden, The Netherlands; <sup>2</sup>Center for Image Sciences, University Medical Centre Utrecht, Utrecht, The Netherlands; <sup>3</sup>Leiden Institute for Brain and Cognition, Leiden University, Leiden, The Netherlands;

<sup>4</sup>Department of Radiology, Leiden University Medical Center, Leiden, The Netherlands; and <sup>5</sup>Department of Pathology, Leiden University Medical Center, Leiden, The Netherlands

Additional supporting information may be found in the online version of this article

This is an open access article under the terms of the Creative Commons Attribution License, which permits use, distribution and reproduction in any medium, provided the original work is properly cited.

gadolinium-based contrast agent (GBCA) and enables assessment of lesion morphology as well as tracer kinetics, both important features for lesion characterization.<sup>6</sup> However, an alternative technique that does not require GBCA injection is desirable because of growing concern related to the use of GBCAs,<sup>7</sup> the additional staff costs because of the time required for intravenous injection,<sup>8</sup> costs of the contrast agent itself,<sup>8</sup> and patient discomfort.

In conventional DCE-MR, both the wash-in and wash-out phase, minutes after contrast administration, are assessed. Studies on ultrafast DCE, with a temporal resolution of seconds in the intravenous contrast wash-in phase, showed similar results in less time.<sup>9,10</sup> The early wash-in phase is mainly determined by perfusion. Later on image contrast is dominated by leakage of the contrast agent into the extravascular space, due to increased vessel wall permeability in tumors.<sup>11</sup>

Arterial spin labeling (ASL) might be a promising noncontrast-enhanced alternative for DCE-MRI. Similar as ultrafast DCE-MRI, ASL provides information on perfusion and vascularity, without being sensitive to vessel wall permeability. However, ASL does not require administration of contrast agent. ASL achieves perfusion contrast by labeling blood magnetically.<sup>12</sup> In ASL, two images are acquired alternately; a label image, where blood is labeled magnetically, and a control image. The label and control images are subtracted to obtain an ASL image, where the static tissue signals cancel out and only labeled blood signal is left. Most common ASL techniques in brain and body, such as pseudo continuous ASL (pCASL),<sup>13,14</sup> and flow-sensitive alternating inversion recovery (FAIR),<sup>15,16</sup> are spatially selective. In spatially selective techniques, labeling of blood takes place in the feeding arteries of the tissue of interest,<sup>12</sup> resulting in a transit delay between the labeling location and arrival of labeled blood in the tissue. During the transit delay, labeled blood will not only flow from the labeling location into the tissue but will also decay with the  $T_1$  of blood, which is around 1.65 sec at 3 T.<sup>14</sup> Thus for a delay of 1.65 sec, already 65% of ASL signal is lost. This poses a significant challenge for breast ASL. Blood flow in the internal mammary artery, feeding the breast is on the order of 19 cm/sec,<sup>17</sup> which is lower than the blood flow in the carotid arteries feeding the brain, that is, 39 cm/sec.<sup>18</sup> This complicates the use of spatially selective ASL techniques in breast.

Velocity-selective ASL is an ASL-technique that labels blood based on flow velocity instead of spatial location.<sup>19</sup> All blood above a certain cutoff velocity gets labeled, so if the cutoff velocity is chosen low enough the transit delay is essentially eliminated. Hence, we hypothesized that VS-ASL can be used in breast and has the potential to serve as a noncontrast-enhanced perfusion method in breast cancer patients.

In this study, the technical feasibility of VS-ASL in breast was investigated. Thus, the aim of this study was to investigate whether VS-ASL generated enough contrast at a lesion location to identify increased perfusion and vascularity within breast lesions compared to surrounding tissue.

## Materials and Methods

### Subjects

This study was approved by the local ethics committee (METC Leiden Den Haag Delft NL70510.058.19) and informed consent was obtained from all participants. Patients were recruited via the outpatient clinic for breast cancer. Inclusion criteria were: scheduled for an MRI breast exam (either for screening or staging purposes), aged 18 years or over, and mentally competent. Exclusion criteria were: unable or unwilling to comply with breathing instructions, contraindications for gadolinium-based contrast agents, and having previously undergone breast reduction treatment.

### Image Acquisition

All subjects were scanned in prone position on a 3 T Philips Ingenia Elition scanner (Philips, Best, The Netherlands), using a dedicated 16-channel bilateral breast coil. For all scans, image-based shimming (SmartBreast, Philips, Best, The Netherlands) was used to reduce  $B_0$ -related artifacts. A VS-ASL and  $M_0$  scan were acquired prior to the standard clinical protocol. To reduce motion artifacts, the VS-ASL and  $M_0$  scans were acquired with paced breathing; patients were asked to synchronize their breathing with image acquisition such that they held their breath (on exhalation) during the acquisition and then took shallow breaths in and out between acquisitions. Coaching was provided via the intercom, and patient cooperation was monitored using VitalEye (Philips, Best, The Netherlands).

The VS-ASL scan was acquired with a single-shot GE-EPI readout.

Twenty transverse slices with 5 mm thickness, a 1 mm slice gap, an acquisition resolution of  $2.75 \times 2.75 \text{ mm}^2$ . The field-of-view was bilateral and was set to  $200 \times 119 \times 196 \text{ mm}^3$ . The scan had a TE of 15 msec, and the TR was set to 6500 msec to produce a close-to-natural breathing rhythm. The fold-over direction was right-left to prevent fold-in signal of the heart. VS-ASL labeling was performed using a pair of hyperbolic secant pulses and bipolar gradients, as described by Wong,<sup>12</sup> using only a single VS-ASL labeling module (i.e. excluding the second VS-ASL labeling module). The VS-ASL scans were acquired with a cutoff velocity of 2 cm/sec, velocity-encoding direction feet-head, VS-ASL module duration of 50 msec, and hyperbolic secant pulses with a maximum  $B_1$  of  $13.5 \mu\text{T}$  and a duration of 20 msec. The postlabel delay (PLD) was set to 1000 msec. Spectral presaturation with inversion recovery (SPIR)<sup>20</sup> fat suppression was used, and background suppression pulses<sup>14</sup> (hyperbolic secant), aimed to null fat signal, were applied 366 msec and 820 msec after labeling. Twenty-one pairs of control and labeled images were acquired, resulting in a scan duration of 4 minutes 46 sec.

An  $M_0$  scan was acquired for calibration of the ASL signal. The  $M_0$  scan was acquired using the same readout as the VS-ASL scan but with ASL labeling turned off. Four

repetitions of the  $M_0$  image were acquired, resulting in a total scan time of 40 sec.

The clinical protocol included  $T_2$ -weighted turbo spin echo (TSE) Dixon, diffusion-weighted imaging (DWI), DCE, and ultrafast DCE scans. The  $T_2$ -weighted Dixon was acquired with 83 slices, an acquisition resolution of  $1.2 \times 1.2 \times 2.4 \text{ mm}^3$ , TE/TR of 140 msec/5856 msec, and a TSE-factor of 24. DWI was acquired with b-values of 500  $\text{s/mm}^2$ , 1000  $\text{s/mm}^2$ , and 1500  $\text{s/mm}^2$ , 42 slices, an acquisition resolution of  $2 \times 2 \times 4 \text{ mm}^3$ , and a 2D SE-EPI readout. Lastly, DCE and ultrafast DCE images were acquired with Dotarem (0.5 mmol/mL) as GBCA, using a dosage of 0.2 cc/kg. Ultrafast DCE was acquired with a 3D gradient-echo  $T_1$ -weighted readout without fat suppression, using 136 slices and a spatial resolution of  $1.3 \times 1.3 \times 1.3 \text{ mm}^3$ . DCE-MRI was acquired using a 3D multishot turbo-field echo (TFE) readout, using a TFE factor of 30, spectral attenuated inversion recovery (SPAIR)<sup>21</sup> fat suppression, 140 slices, and a spatial resolution of  $1.0 \times 1.0 \times 1.5 \text{ mm}^3$ . Before contrast injection, baseline DCE and ultrafast DCE-images were acquired. Directly after contrast injection, the ultrafast DCE series of 14 time points with a temporal resolution of 3.9 s was started, and subsequently the regular DCE-series of five time points with a temporal resolution of 1 minute 12 sec.

### Image Analysis

Image analysis was performed using MeVisLab (MeVis Medical Solutions AG, Fraunhofer MEVIS, Bremen, Germany). The breast VS-ASL and  $M_0$  images were co-registered to each other using a group-wise image registration method.<sup>22</sup> For each voxel  $i$ , the ASL subtraction signal  $\Delta S_i$  was obtained by subtracting control ( $C_{r,i}$ ) and label ( $L_{r,i}$ ) images, and averaged over the total number of repetitions  $R$  (Eq. 1). An  $M_0$ -value was obtained by averaging over all  $N$  voxels within a manually drawn ROI<sub>heart</sub> (researcher S.L.F in consensus with radiologist N.V.) in the left ventricle of the heart (Eq 2). The resulting perfusion-weighted signal (PWS) value for each voxel  $i$  was obtained by dividing the ASL images with the  $M_0$ -value.

$$\Delta S_i = \frac{1}{R} \sum_{r=1}^R (C_{r,i} - L_{r,i}) \quad (1)$$

$$M_0 = \frac{1}{N} \sum_{i_{ROI-\text{heart}}=1}^N M_{0,i_{ROI-\text{heart}}} \quad (2)$$

$$PWS_i = \frac{\Delta S_i}{M_0} \quad (3)$$

Scans from the standard clinical protocol were assessed as part of the standard clinical protocol. In case a lesion was present, information regarding location, size, apparent diffusion coefficient (ADC) map reduction, and whether the lesion presents itself as mass (space-occupying) or nonmass

(areas of enhancement without clear space-occupancy) according to the BI-RADS lexicon<sup>23</sup> was extracted from the clinical report. In addition, images from the clinical DCE, ultrafast DCE scans and the ADC maps calculated from the clinical DWI-scans were obtained from the clinical patient database. Ultrafast DCE images at 10 sec after enhancement of internal thoracic artery, reflecting mainly perfusion, were obtained to compare to the VS-ASL images. All patients included for staging purposes received a biopsy prior to MRI, while all patients included for screening purposes only received a biopsy post-MRI in case there was an indication based on the MRI results. When available, lesion characterization from biopsy was obtained from the clinical reports.

Three radiologists (N.V./T.K./M.N.J.M.W.) with 3–25 years of experience in breast radiology scored the PWS-maps of the VS-ASL scans on lesion visibility and artifacts, based on a 3-point Likert scale. For lesion visibility, a score of 1 was defined as: “signal at the location of the lesion can be distinguished from surrounding tissue,” 2: “suspicion that signal at the location of the lesion is deviant from surrounding tissue,” 3: “signal at the location of the lesion cannot be distinguished from surrounding tissue.” For the artifact score, a score of 1 was defined as: “no or few artifacts are visible, artifacts can be distinguished from blood signal,” 2: “artifacts are visible, most can be distinguished from blood signal,” and 3: “artifacts have similar intensity as blood signal, and obscure assessment of the image.”

In addition, ROIs were drawn at the location of the lesion (in all slices occupied by the lesion) by a researcher (S.L.F) in consensus with a radiologist (N.V.). The PWS values of all  $J$  voxels in the ROI were averaged, to obtain a measure for signal enhancement of the lesion ( $PWS_{\text{lesion}}$ ) on the VS-ASL PWS images (see Eq. 4).

$$PWS_{\text{lesion}} = \frac{1}{J} \sum_{i_{ROI-\text{lesion}}=1}^J PWS_{i_{ROI-\text{lesion}}} \quad (4)$$

### Histopathology

Microscopic evaluation of the tissue was performed for two patients (patients 2 and 7). One of the two patients underwent preventive bilateral breast ablation, and the other patient underwent lumpectomy. Thin section histopathology slices were analyzed to evaluate vascularity around the lesions, to be able to check for a biological basis of the VS-ASL signal observed in these two patients.

### Statistical Analysis

The intra-class correlation coefficient (ICC) was calculated to assess inter-observer agreement, using SPSS Statistics (IBM Corp, Armonk, NY, USA), using a significance level of 0.05.

An ICC of  $>0.74$  was considered excellent, 0.6–0.74 good, 0.4–0.59 fair, and  $<0.4$  poor.

## Results

Preliminary data comparing VS-ASL with a SE-EPI and GE-EPI readout, and comparing multislice VS-ASL with FAIR, a spatially selective technique, acquired with a single as well as a multislice readout is presented in Figs. 1, 2 and 3 in the Supplemental Material. Based on the standard clinical protocol, 7 out of 10 patients had a lesion on DCE-MRI, of which one patient had bilateral lesions (Table 1). Four lesions were classified as invasive carcinoma, three as DCIS and one as a benign blunt duct adenosis. In one patient (patient 3), the lesion was not visible on DCE-MRI, since it was a small focus of DCIS grade 1, which was likely completely removed by biopsy prior to the MRI. Of these eight lesions visible on DCE-MRI, five presented as mass, with sizes ranging between 23 and 32 mm, and three as nonmass, with sizes ranging between 10 and 12 mm.

There was an excellent inter-observer agreement between the three readers for lesion visibility (ICC = 0.77, 95% confidence interval [CI] = 0.18–0.95) and artifact scoring (ICC = 0.84, IC = 0.55–0.95). Table 1 shows for all patients: the outcomes of the clinical MR exam, biopsy results, mean PWS of the lesion, and the lesion visibility and artifact scores averaged over the three observers. The mean lesion visibility score was 1.58. Mass lesions had a mean score of 1.27 and nonmass lesions 2.11.

Overall, VS-ASL showed a comparable morphology to the early time point of ultrafast DCE. Larger arteries and veins were also clearly visualized. A representative patient with bilateral mass lesions is shown in Fig. 1, and a representative patient with nonmass lesions in Fig. 2.

The mean artifact score was 1.9. Mass lesions had a mean artifact score of 1.53, and nonmass lesions 2.11. A representative patient with a high artifact score is shown in Fig. 3.

While scoring the data, an observation was made (N.V.) concerning increased VS-ASL signal adjacent to the lesion, which was consistent with a segmental pattern. This segmental pattern of increased VS-ASL signal was observed in three patients, see Fig. 4 for a representative case. No correlate was found on the ultrafast DCE images for these findings. However, on the DCE images, all three patients have notable vessels in these areas, see Fig. 4(c).

Histopathological analyses were performed for two patients: one diagnosed with a DCIS lesion (patient 2) and one with an invasive carcinoma (patient 7), see Table 1. In both patients, a clear difference in the size and hypertrophy of the small vessels surrounding the lesion, compared to the healthy breast tissue in the same patient was observed, see Fig. 4 in the Supplemental Material.

## Discussion

Our results demonstrated the feasibility of bilateral whole-breast perfusion imaging using VS-ASL in breast cancer patients. Moreover, a correspondence was observed in morphology of the patterns seen in VS-ASL and early-phase ultrafast DCE images.

Finding a noncontrast imaging technique to investigate tumor perfusion and vascularity is essential, as angiogenesis is one of the first signs of tumor growth and is critical for identifying breast cancers with a higher potential for invasion and metastasis.<sup>24,25</sup> Compared to traditional ASL methods, VS-ASL addresses the challenging perfusion characteristics of the breast and enables bilateral whole-breast perfusion imaging.

Previous studies investigating the feasibility of ASL in breast cancer employed spatially selective ASL techniques with a single slice planned on the tumor, using coronal slices to label the chest wall including the heart.<sup>26–29</sup> However, spatially selective ASL can lead to low SNR in case of multislice scanning in breast, due to slow flow. When using a multislice readout, the label is created further away from the breast tissue and the resulting prolonged transit delays, due to slow flow, will result in little label having reached the relevant slices at the time of acquisition. If the PLD is adjusted to for the prolonged transit delays, more SNR would be lost to  $T_1$ -decay of label, leading to poor image quality. Moreover, single-slice FAIR would have, in addition to arterial signal, a contribution from venous signal flowing in posterior direction. Because whole-breast coverage is a necessity for screening purposes, spatially selective ASL is unsuitable as a noncontrast screening method.

Overall, interobserver agreement of VS-ASL was excellent for lesion visibility, and the artifact score. The mean lesion visibility was good, indicating that signal at the lesion could either be clearly distinguished from surrounding tissue or that there was a suspicion that the signal was deviant at the location of the lesion. The results suggest that in this limited sample size, nonmass lesions were less visible. However, the non-mass lesions included in this study also had a smaller size. Visibility of the lesions on VS-ASL corresponded well with visibility on the early phase ultrafast DCE images, confirming that VS-ASL is a measure of perfusion and vascularity, similar to early phase ultrafast DCE.<sup>11</sup> Parameters derived from ultrafast DCE-MRI have been shown to be able to discriminate between benign and malignant lesions<sup>30</sup> and have a strong relationship with tumor subtype.<sup>31</sup> Thus, it would be interesting to investigate whether VS-ASL could also provide sufficient information to discriminate between benign and malignant lesions.

While scoring the data, there was an unexpected finding by one of the observers: segmental patterns of increased perfusion were observed on the VS-ASL PWS images adjacent to the lesion for three patients. In all cases, the pattern followed

**TABLE 1. Patient Characteristics and Results of Clinical MR Exam, Biopsy, and the Velocity-Selective Arterial Spin Labeling (VS-ASL) Scan**

Patient	Left/Right Breast	Clinical MR Exam				Biopsy		VS-ASL		VS-ASL: Mean scores observers	
		Indication	Size (mm)	DCE-Enhancement	ADC Reduction	Hormone Receptors	Lesion type	PWS at lesion (%M0)	Lesion visibility	Artifact	
1	-	Screening	-	-	-	-	-	-	-	-	2
2	Left	Screening	11	Non-mass	Yes	-	DCIS 2	0.50	2	2	2
3	Left	Staging	6	Not visible <sup>a</sup>	No	-	DCIS 1	-	-	-	2.6
4	-	Screening	-	-	-	-	-	-	-	-	2.3
5	Left	Staging	27	Mass	Yes	ER+, PR-, HER2- (right)	DCIS 1 + adenosis	0.70	1.3	2	2
	Right		32	Mass	Yes	-	Invasive lobular carcinoma 2	0.32	1	1.3	
6	Right	Staging	30	Mass	Yes	ER+, PR-, HER2-	Invasive carcinoma NST 2	0.76	1	1	1
7	Left	Staging	23	Mass	Yes	ER+, PR+, HER2+	Invasive carcinoma NST 2	0.78	1	1	1
8	Right	Staging	12	Non-mass	No	ER-, PR-, HER2-	Invasive carcinoma NST 3	0.17	2.3	2.3	2.3
9	Right	Staging	10	Non-mass	Yes	-	Blunt duct adenosis	0.4	2	2	2
10	Left	Staging	33	Mass	Yes	ER+, PR-, HER2-	Pleiomorphic lobular carcinoma	3.34	2	2.3	2.3

<sup>a</sup>DCIS grade1 was found in a stereotactic biopsy specimen of 4 mm suspicious calcifications, in which probably the whole lesion was removed. The results presented for the clinical MR exam and biopsy were taken from the clinical report. DCE = dynamic contrast enhanced, ADC = apparent diffusion coefficient, ER± = estrogen receptor positive/negative, PR± = progesterone receptor positive/negative, HER2± = human epidermal growth factor receptor-2 positive/negative, DCIS = ductal carcinoma in-situ, PWS = perfusion-weighted signal, Lesion visibility; 1 = "signal at the location of the lesion can be distinguished from surrounding tissue," 2 = "suspicion that signal at the location of the lesion is deviant from surrounding tissue," 3 = "signal at the location of the lesion cannot be distinguished from surrounding tissue." Artifact score; 1 = "no or few artifacts are visible, artifacts can be distinguished from blood signal," 2 = "artifacts are visible, most can be distinguished from blood signal," 3 = "artifacts have similar intensity as blood signal, and obscure assessment of the image."

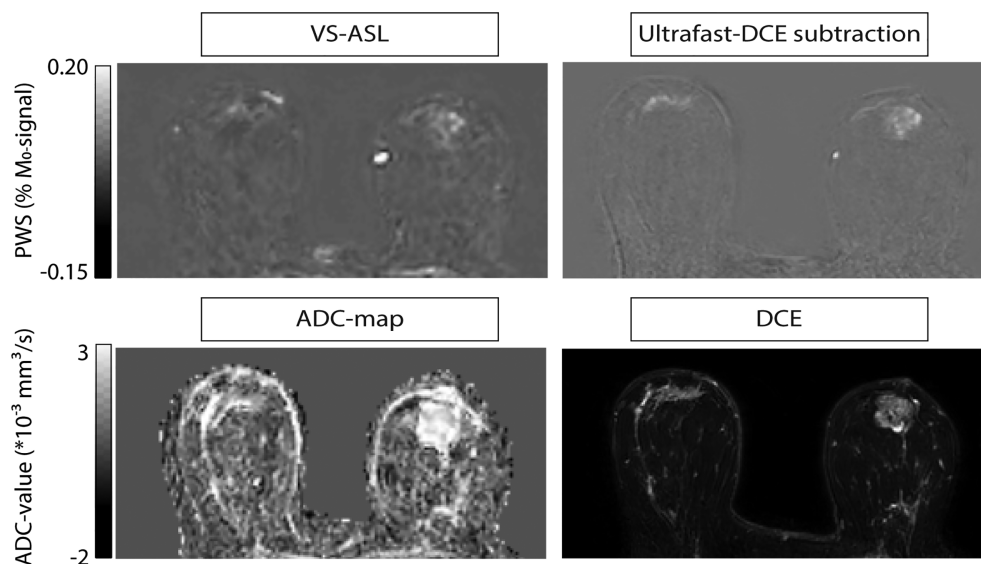


**FIGURE 1:** Representative patient with mass lesions; patient 5 with invasive lobular carcinoma grade 2 in right breast, and ductal carcinoma in situ grade 1 with adenosis in left breast. Signal in the VS-ASL image corresponds with perfusion signal in early-phase ultrafast DCE. Top row, from left to right: VS-ASL, and the subtraction image of ultrafast DCE at a time point of 10 sec after contrast agent arrival in the internal thoracic artery. Bottom row, from left to right: ADC map calculated from  $b = 500\text{--}1000$  s/mm<sup>2</sup> and the first time point after contrast injection of the standard DCE scan, reflecting both perfusion and vessel wall permeability.

prominent vessels which were visible on DCE-MR, suggesting a biological basis for the segmental perfusion patterns. The segmental perfusion patterns could indicate increased flow in the drainage area of the lesion due to a pathological vascular bed. Because vascularization has shown to be valuable in tumor diagnosis,<sup>32,33</sup> it would be interesting to investigate whether vascularization scores and observation of segmental perfusion patterns can aid detection of lesions in VS-ASL images.

Scoring of the artifacts showed that artifacts were present in the VS-ASL data, but that, overall, they could be distinguished from blood signal. In a few cases, the mean artifact score indicated that artifacts impacted proper assessment of the image. In all of these cases, the patient had extremely dense breast, according to the American College of Radiology classification, except for one patient who had a blood edema next to the lesion which obscured visibility. The artifacts observed in patients with dense breast are likely a result of a

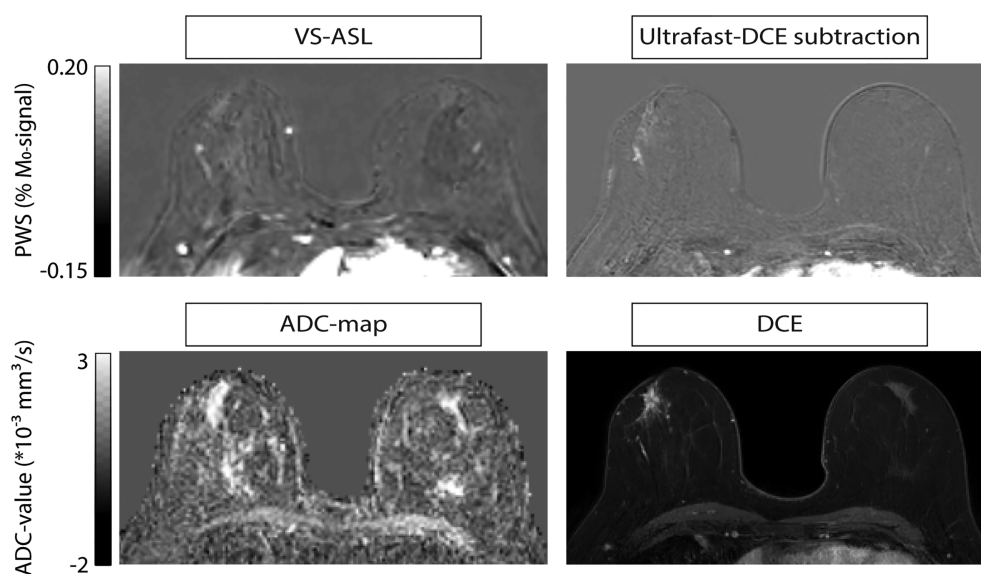


**FIGURE 2:** Representative patient with a non-mass lesion; patient 9 with adenosis in the right breast. Signal in the VS-ASL images corresponds with perfusion signal in the early phase ultrafast DCE. Top row, from left to right: VS-ASL, and the subtraction image of ultrafast DCE at a time point of 10 sec after contrast agent arrival in the internal thoracic artery. Bottom row, from left to right: ADC map calculated from  $b$  500–1000 sec/mm<sup>2</sup>, and the first time point approximately 1 minute after contrast injection of the standard DCE scan, reflecting both perfusion and vessel wall permeability.

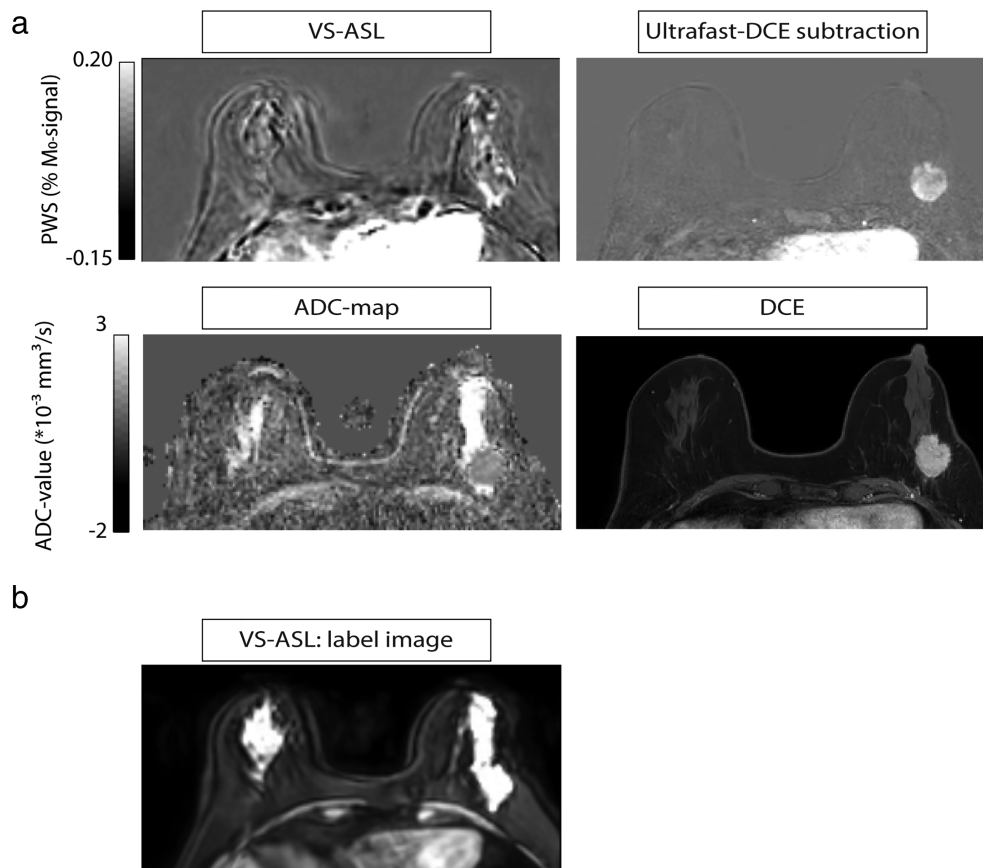


**FIGURE 3:** Representative patient with dense breast; (a) patient 10 with a pleiomorphic lobular carcinoma in the left breast, and dense breast. (b) The dense glandular tissue gives a relatively high signal contrast on the label images. Thus, motion can consequently easily lead to subtraction errors in the VS-ASL image.

high contrast between fat and glandular tissue in the raw VS-ASL images, which can easily lead to subtraction artifacts in case of small movements. Currently, two background suppression pulses were used. The short PLD of VS-ASL prevents optimal suppression of both fat and glandular tissue. Possible strategies to improve the background suppression would be to increase the PLD and optimize timings for both tissue types, or to increase the number of background suppression pulses to three, to be able to suppress tissues across a broader range of  $T_1$  values.<sup>34</sup> However, both strategies would come at the cost of SNR, by increased  $T_1$ -decay or by increased signal loss due to imperfect inversion pulses, respectively. Future studies are necessary to find out whether these proposed strategies result in a reduction of subtraction artifacts in patients with dense breast, at an acceptable SNR penalty.

Note that the VS-ASL signal we measured is a combination of arterial and venous signal. Single VS-ASL was used: meaning that only one VS-ASL module was applied, instead of two as is commonly done in VS-ASL.<sup>19</sup> This second labeling module acts as a vascular crusher with a matched cutoff velocity, in both label and control condition. It has the effect of removing the venous and vascular contributions to the

signal and defines the bolus duration, such that quantification of perfusion becomes possible. However, it comes at the expense of a reduction in SNR.<sup>35</sup> This module was not applied by us, because being able to visualize venous and vascular signal could be clinically relevant in breast cancer patients, and, because we opted for maximum SNR for these first applications of VS-ASL in breast, in view of the anticipated low ASL signal.

The single VS-ASL sequence was played out with a cutoff velocity of 2 cm/sec, as has previously been done,<sup>19</sup> while using a relatively short PLD. The choice of cutoff velocity is a trade-off between labeling as close as possible to target tissue while preventing imaging artifacts caused by the increased gradient area. The motivation for using a short PLD was 2-fold. First, the low cutoff velocity provides label already within the target region. Second, single VS-ASL was used, that is, there is no second VS-ASL labeling module. Conventionally in VS-ASL, a longer PLD is required to ensure deceleration of the labeled blood before the second VS-ASL module is applied. In our implementation, this was not the case, so a shorter PLD was used to prevent unnecessary loss of ASL-signal due to  $T_1$ -decay.

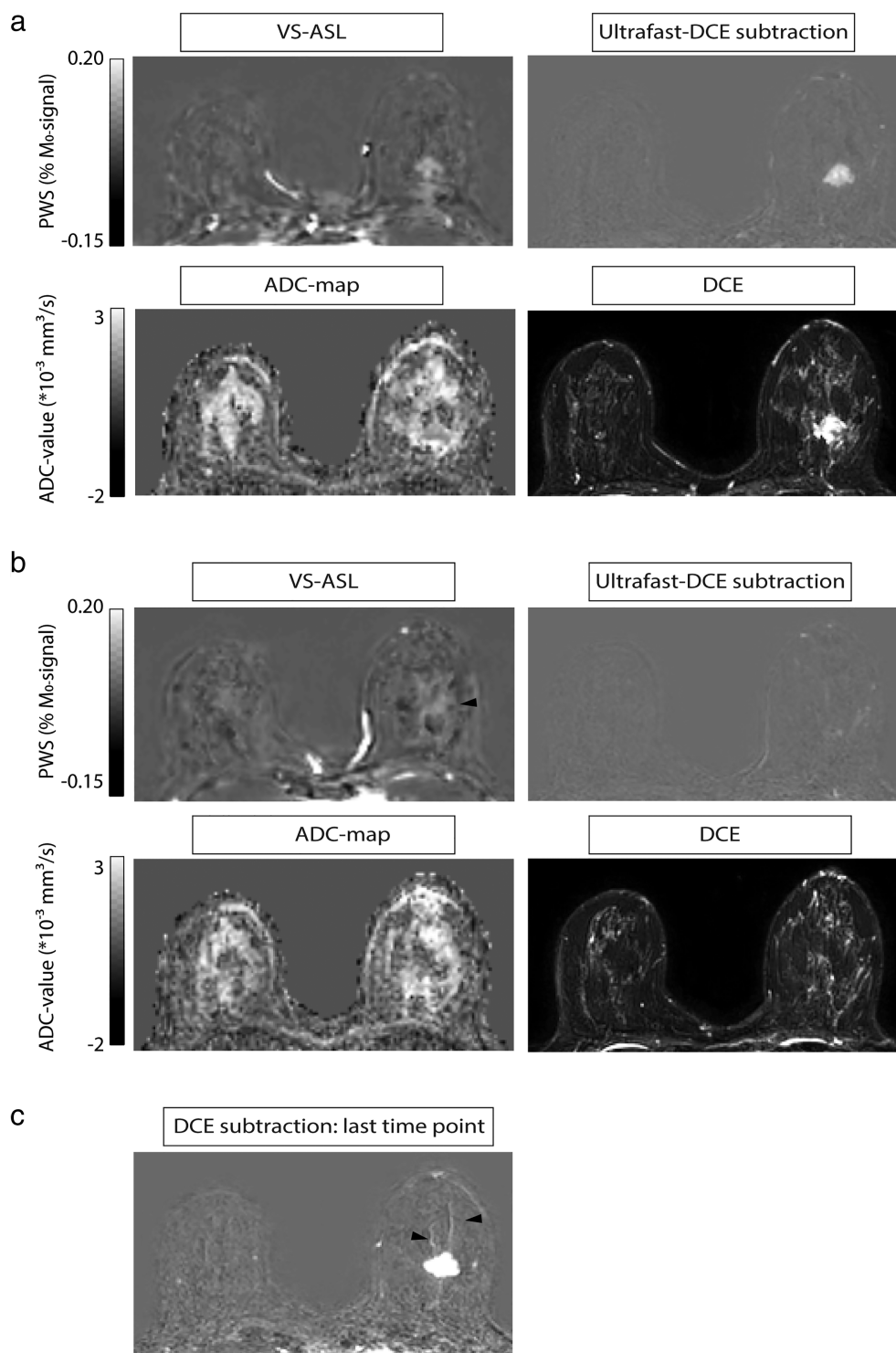


**FIGURE 4:** Representative patient with a segmental pattern of increased VS-ASL signal; patient 7 with an invasive carcinoma grade 2 in the right breast. (a) slice containing the lesion, signal in the VS-ASL image corresponds with perfusion signal in the early-phase ultrafast DCE. (b) Segmental pattern of increased perfusion (indicated by black arrow) on the VS-ASL images, in an adjacent slice to the tumor. There is no correlate of this pattern on the DCE, ultrafast DCE or the ADC map. However, in (c) notable vessels (indicated by black arrows) in the same area can be seen on the last time point of the DCE subtraction, likely showing a biological basis for the perfusion pattern seen in b. Histopathological data of this patient is shown in Supporting Information Fig. 4. Within sections A and B: Top row, from left to right: VS-ASL, and the subtraction image of ultrafast DCE at a time point of 10 sec after contrast agent arrival in the internal thoracic artery. Bottom row, from left to right: ADC map calculated from  $b = 500\text{--}1000\text{ sec/mm}^2$ , and the first time point after contrast injection of the standard DCE scan, reflecting both perfusion and vessel wall permeability.



Histopathologic analyses confirmed more vessels as well as more hypertrophic vessels at the border of a DCIS grade 2 and an invasive carcinoma, providing a possible biological basis for the VS-ASL signal. Vascularity is an important characteristic of biologically more aggressive breast cancer subtypes.<sup>32,33</sup> Sensitive to vascularization and perfusion, VS-ASL may also be sensitive to biologically aggressive breast cancer subtypes, similar as DCE-MRI.<sup>36</sup>

### Limitations

First, as mentioned above, the background suppression should be optimized to reduce subtraction artifacts in patients with dense breast. Second, larger voxel sizes were used for VS-ASL ( $2.75 \times 2.75 \times \text{mm}^3$ ) compared to DCE-MRI ( $1 \times 1 \times 1.5 \text{ mm}^3$ ) and ultrafast DCE ( $1.3 \times 1.3 \times 3 \text{ mm}^3$ ), and since the desired detection limit of DCE-MRI is 5 mm,<sup>6</sup> future studies are needed to determine whether that detection limit can be met by VS-ASL.

Third, in contrast to DCE-MRI, no information on kinetics and vessel wall permeability is acquired with VS-ASL. These parameters are currently used to differentiate between lesion subtypes; however, studies using ultrafast DCE-MRI have shown that similar diagnostic accuracy can be achieved by only looking at the early perfusion phase, which does not include information on vessel wall permeability.<sup>30,31</sup> Future studies are necessary to investigate whether VS-ASL could provide similar information as ultrafast DCE and whether other characteristics in VS-ASL images could provide the same, or at least sufficient, discriminatory capability. Fourth, the VS-ASL technique we used may not be the optimal velocity-selective technique. For example, symmetric BIR-8 VS-ASL would be an interesting approach to limit erroneous labeling due to eddy currents and achieve higher robustness to  $B_0$  and  $B_1$ .<sup>37</sup> Also velocity-selective prepared inversion (VSI-) ASL, which has demonstrated similar SNR as pCASL,<sup>38,39</sup> would be an interesting option. An adaptation to the original VSI-ASL sequence has been published to improve the robustness for  $B_0$  and  $B_1$ ,<sup>40</sup> which could prove essential for breast applications. Finally, the aim of this study was to do a technical proof-of-concept, so a small sample group was included. Future studies should include larger patient groups to establish the sensitivity and specificity of this technique, in terms of specific populations as well as lesion size and cancer subtype.

### Conclusion

Our results demonstrate the feasibility of VS-ASL as a noncontrast-enhanced measurement of perfusion and vascularity in breast. VS-ASL is a promising technique that could add to a noncontrast mpMRI protocol for breast. A noncontrast mpMRI protocol would considerably reduce both patient discomfort and cost and could possibly be used as a

prescreening method so that only patients with suspicious findings are referred for a DCE-MRI exam.

### Acknowledgments

The authors thank MeVis Medical Solutions AG (Bremen, Germany) for providing MeVisLab medical image processing and visualization environment, which was used for image analysis. The authors thank E. M. M. Krol-Warmerdam, J. van Leeuwen-Büttner, and G.M.C. Ranke for their valuable help in recruitments of patients. This work is part of the research program Drag and Drop ASL with project number 14951, which is (partly) financed by the Netherlands Organization for Scientific Research (NWO).

### References

- Mann RM, Kuhl CK, Moy L. Contrast-enhanced MRI for breast cancer screening. *J Magn Reson Imaging* 2019;50:377-390.
- Marino MA, Helbich T, Baltzer P, Pinker-Domenig K. Multiparametric MRI of the breast: A review. *J Magn Reson Imaging* 2018;47(2):301-315.
- Saslow D, Boetes C, Burke W, et al. American Cancer Society guidelines for breast screening with MRI as an adjunct to mammography. *CA Cancer J Clin* 2007;57(2):75-89.
- Antoniou A, Pharoah PDP, Narod S, et al. Average risks of breast and ovarian cancer associated with BRCA1 or BRCA2 mutations detected in case series unselected for family history: A combined analysis of 22 studies. *Am J Hum Genet* 2003;72(5):1117-1130.
- Chen S, Parmigiani G. Meta-analysis of BRCA1 and BRCA2 penetrance. *J Clin Oncol* 2007;25(11):1329-1333.
- Mann RM, Cho N, Moy L. Breast MRI: State of the art. *Radiology* 2019;292(3):520-536.
- McDonald RJ, Levine D, Weinreb J, et al. Gadolinium retention: A research roadmap from the 2018 NIH/ACR/RSNA workshop on gadolinium chelates. *Radiology* 2018;289(2):517-534.
- for the UK Magnetic Resonance Imaging in Breast Screening (MARIBS) Study Group, Griebisch I, Brown J, et al. Cost-effectiveness of screening with contrast enhanced magnetic resonance imaging vs X-ray mammography of women at a high familial risk of breast cancer. *Br J Cancer* 2006;95(7):801-810.
- Abe H, Mori N, Tsuchiya K, et al. Kinetic analysis of benign and malignant breast lesions with ultrafast dynamic contrast-enhanced MRI: Comparison with standard kinetic assessment. *Am J Roentgenol* 2016;207(5):1159-1166.
- van Zelst JCM, Vreemann S, Witt HJ, et al. Multireader study on the diagnostic accuracy of ultrafast breast magnetic resonance imaging for breast cancer screening. *Investigative Radiology* 2018;53(10):579-586.
- Gao Y, Heller SL. Abbreviated and ultrafast breast MRI in clinical practice. *Radiographics* 2020;40(6):1507-1527.
- Wong EC. An introduction to ASL labeling techniques. *J Magn Reson Imaging* 2014;40(1):1-10.
- Dai W, Garcia D, de Bazelaire C, Alsop DC. Continuous flow-driven inversion for arterial spin labeling using pulsed radio frequency and gradient fields. *Magn Reson Med* 2008;60(6):1488-1497.
- Alsop DC, Detre JA, Golay X, et al. Recommended implementation of arterial spin-labeled perfusion MRI for clinical applications: A consensus of the ISMRM perfusion study group and the European consortium for ASL in dementia. *Magn Reson Med* 2015;73(1):102-116.
- Kim S-G. Quantification of relative cerebral blood flow change by flow-sensitive alternating inversion recovery (FAIR) technique: Application to functional mapping. *Magn Reson Med* 1995;34(3):293-301.

16. Nery F, Buchanan CE, Hartevelde AA, et al. Consensus-based technical recommendations for clinical translation of renal ASL MRI. *Magn Reson Mater Phy* 2020;33:141-161.
17. Korovessis P, Iliopoulos P, Misiris A, Koureas G. Color Doppler ultrasonography for evaluation of internal mammary artery application in adolescent female patients with right-convex thoracic idiopathic scoliosis. *Spine (Phila pa 1976)* 2003;28(15):1746-1748.
18. Holdsworth DW, Norley CJD, Frayne R, Steinman DA, Rutt BK. Characterization of common carotid artery blood-flow waveforms in normal human subjects. *Physiol Meas* 1999;20(3):219-240.
19. Wong EC, Cronin M, Wu WC, Inglis B, Frank LR, Liu TT. Velocity-selective arterial spin labeling. *Magn Reson Med* 2006;55(6):1334-1341.
20. Kaldoudi E, Williams SCR, Barker GJ, Tofts PS. A chemical shift selective inversion recovery sequence for fat-suppressed MRI: Theory and experimental validation. *Magn Reson Imaging* 1993;11(3):341-355.
21. Lauenstein TC, Sharma P, Hughes T, Heberlein K, Tudorascu D, Martin DR. Evaluation of optimized inversion-recovery fat-suppression techniques for T2-weighted abdominal MR imaging. *J Magn Reson Imaging* 2008;27(6):1448-1454.
22. Huizinga W, Poot DHJ, Guyader JM, et al. PCA-based groupwise image registration for quantitative MRI. *Med Image Anal* 2016;29:65-78.
23. D'Orsi C, Sickles E, Mendelson E, Morris E. *Breast Imaging Reporting and Data System: ACR BI-RADS breast imaging atlas*. 5th ed. Reston: American College of Radiology; 2013.
24. Hanahan D, Folkman J. Patterns and emerging mechanisms review of the angiogenic switch during tumorigenesis. *Cell* 1996;86:353-364.
25. Hanahan D, Weinberg RA. Hallmarks of cancer: The next generation. *Cell* 2011;144(5):646-674.
26. Wu, W-C, England, S, Schnall M, Wang, J. Feasibility of arterial spin labeling in the measurement of breast perfusion, 2007.
27. Kawashima M, Katada Y, Shukuya T, Kojima M, Nozaki M. MR perfusion imaging using the arterial spin labeling technique for breast cancer. *J Magn Reson Imaging* 2012;35(2):436-440.
28. Han M, Hargreaves BA, Daniel BL, et al. Breast perfusion imaging using arterial spin labeling. *Proceedings International society of magnetic resonance in imaging* 2010;18:2501-2501.
29. Buchbender S, Obenauer S, Mohrmann S, et al. Arterial spin labelling perfusion MRI of breast cancer using FAIR TrueFISP: Initial results. *Clin Radiol* 2013;68(3):e123-e127.
30. Goto M, Sakai K, Yokota H, et al. Diagnostic performance of initial enhancement analysis using ultra-fast dynamic contrast-enhanced MRI for breast lesions. *Eur Radiol* 2019;29(3):1164-1174.
31. Onishi N, Sadinski M, Hughes MC, et al. Ultrafast dynamic contrast-enhanced breast MRI may generate prognostic imaging markers of breast cancer. *Breast Cancer Res* 2020;22(1):58.
32. Schmitz AC, Peters NHGM, Veldhuis WB, et al. Contrast-enhanced 3.0-T breast MRI for characterization of breast lesions: Increased specificity by using vascular maps. *Eur Radiol* 2008;18(2):355-364.
33. Wu C, Pineda F, Hormuth DA, Karczmar GS, Yankeelov TE. Quantitative analysis of vascular properties derived from ultrafast DCE-MRI to discriminate malignant and benign breast tumors. *Magn Reson Med* 2019;81(3):2147-2160.
34. Mani S, Pauly J, Conolly S, Meyer C, Nishimura D. Background suppression with multiple inversion recovery nulling: Applications to projective angiography. *Magn Reson Med* 1997;37(6):898-905.
35. Schmid S, Ghariq E, Teeuwisse WM, Webb A, van Osch MJP. Acceleration-selective arterial spin labeling. *Magn Reson Med* 2014;71(1):191-199.
36. Sung JS, Stamler S, Brooks J, et al. Breast cancers detected at screening mr imaging and mammography in patients at high risk: Method of detection reflects tumor histopathologic results. *Radiology* 2016;280(3):716-722.
37. Guo J, Meakin JA, Jezzard P, Wong EC. An optimized design to reduce eddy current sensitivity in velocity-selective arterial spin labeling using symmetric BIR-8 pulses. *Magn Reson Med* 2015;73(3):1085-1094.
38. Qin Q, Shin T, Schär M, Guo H, Chen H, Qiao Y. Velocity-selective magnetization-prepared non-contrast-enhanced cerebral MR angiography at 3 tesla: Improved immunity to B0/B1 inhomogeneity. *Magn Reson Med* 2016;75(3):1232-1241.
39. Franklin SL, Bones IK, Hartevelde AA, et al. Multi-organ comparison of flow-based arterial spin labeling techniques: Spatially non-selective labeling for cerebral and renal perfusion imaging. *Magn Reson Med* 2020;85:2580-2594.
40. Liu D, Li W, Xu F, Zhu D, Shin T, Qin Q. Ensuring both velocity and spatial responses robust to field inhomogeneities for velocity-selective arterial spin labeling through dynamic phase-cycling. *Magn Reson Med* 2020;85(5):2723-2734.